BMB
reports

Different modes of antibiotic action of homodimeric and monomeric bactenecin, a cathelicidin-derived antibacterial peptide

Ju Yeon Lee[1], *Sung-Tae Yang*[1,2], *Hyo Jeong Kim*[1], *Seung Kyu Lee*[1], *Hyun Ho Jung*[1], *Song Yub Shin*[3] *& Jae Il Kim*[1,4,*]

[1]Department of Life Science, Research Center for Bio-imaging, Gwangju Institute of Science and Technology, Gwangju 500-712, Korea, [2]Section on Membrane Biology, Laboratory of Cellular and Molecular Biophysics, National Institute of Child Health and Human Development, National Institutes of Health, Bethesda, MD 20892, USA, [3]Department of Bio-Materials, Graduate School and Department of Cellular & Molecular Medicine, School of Medicine, Chosun University, Gwangju 501-759, [4]AnyGen Co. Ltd., Gwangju 500-712, Korea

The bactenecin is an antibacterial peptide with an intramolecular disulfide bond. We recently found that homodimeric bactenecin exhibits more potent antibacterial activity than the monomeric form and retains its activity at physiological conditions. Here we assess the difference in the modes of antibiotic action of homodimeric and monomeric bactenecins. Both monomeric and dimeric bactenecins almost completely killed both *Staphylococcus aureus* and *E. coli* within 10-30 min at concentrations of 8-16 μM. However, exposure to liposomes elicited an increase in the fluorescence quantum yield from a tryptophan-containing monomeric analog, while the homodimeric analog showed a significant reduction in fluorescence intensity. Moreover, unlike the monomer, the homodimer displayed apparent membrane-lytic activity enabling release of various sized dyes from liposomes, and rapidly and fully depolarized the *S. aureus* membrane. Together, our results suggest that homodimeric bactenecin forms pores in the bacterial membrane, while monomeric one penetrates through the membrane to target intracellular molecules/organelles. [BMB reports 2009; 42(9): 586-592]

INTRODUCTION

A variety of antibacterial peptides with diverse sequences, structures and functions serve as important components of the innate host defense system in living organisms (1-3). Despite their molecular diversity, nearly all of these molecules carry a highly positive net charge and assume an amphipathic tertiary structure, which underlies for their selectivity against bacterial cells (4). Two mechanisms have been proposed to explain the mode of action of antibacterial peptides: 1) permeabilization of the bacterial cytoplasmic membrane and 2) penetration of the cell membrane followed by interaction with intracellular targets (5, 6). In the case of the former, membrane-targeting antibacterial peptides aggregate on the surface of bacterial cells and then penetrate into the lipid membrane to form transmembrane channels or pores (7, 8). In the case of latter, the peptides penetrate all the way through the membrane and then inhibit various intracellular functions, including cell wall, nucleic acid and protein synthesis (9). Interestingly, recent findings suggest that the bactericidal effects of some antibacterial peptides involve a dual mode of action: membrane disruption coupled to secondary intracellular targeting (10, 11).

The antibacterial peptide bactenecin, which is expressed by bovine neutrophils, is a β-hairpin monomer that contains four arginine residues and one intramolecular disulfide bond, and is more potent against Gram-negative than Gram-positive bacteria (12, 13). A similar antibacterial spectrum was previously observed with two other bactenecin family members, Bac5 and Bac7 (14). Most likely, the greater efficacy of these peptides against Gram-negative bacteria mainly reflects their ability to bind to lipopolysaccharides, which are the major constituent of the cell wall of Gram-negative bacteria. On the other hand, the linear, or reduced, form of bactenecin reportedly shows greater bactericidal activity against Gram-positive bacteria (13, 15).

Evidence also suggests that it is the pro-form of bactenecin that is released as a dimer *in vivo* (16). Consistent with that idea, we recently showed that a reduced linear bactenecin preferentially folds into an antiparallel dimeric form via intermolecular disulfide bonding under oxidative folding conditions *in vitro* (17). And in the same study, we showed that the antibacterial activity of homodimeric bactenecin is more effective than that of the monomer, and that the dimeric form retains its bactericidal efficacy at a physiological salt concentration, whereas the monomeric form does not (17). Notably, monomeric bactenecin does not elicit cytoplasmic membrane depolarization in *E. coli* DC2 cells, though its potent bactericidal activity against *E. coli* suggests the monomer crosses the cytoplasmic membrane and acts on intracellular targets (18). Details of the molecular mechanism underlying for bactericidal action of homodimeric bactenecin remain unclear, however.

Because homodimeric bactenecin differs from the mono-

*Corresponding author. Tel: 82-62-970-2494; Fax: 82-62-970-2484; E-mail: jikim@gist.ac.kr

Received 27 March 2009, Accepted 6 April 2009

Keywords: Antibacterial activity, Homodimeric bactenecin, Model membrane, Monomeric bactenecin, Oligomerization

meric form with respect to the number of amino acid residues, structure and antibacterial efficacy, our aim in the present study was to determine whether the mode of action of homodimeric bactenecin is similar to that of the monomeric form. To accomplish this, we designed and synthesized several bactenecin derivatives, including two tryptophan-substituted analogs, and investigated their mode of interaction using bacterial and lipid model membranes.

RESULTS AND DISCUSSION

Peptide design and synthesis

To assess the different modes of antibacterial action of homodimeric and monomeric bactenecins, we designed four derivatives: monomeric turn bactenecin (MTB), tryptophan-substituted monomeric bactenecin (TMB), antiparallel dimeric bactenecin (ADB), and tryptophan-substituted dimeric bactenecin (TDB). In both TDB and TMB we substituted a tryptophan residue for the valine at the center position of the peptide in order to use the spectroscopic properties of tryptophan to evaluate the interaction of the peptides with a model membrane (19). The monomeric bactenecins MTB and TMB, which contain an intramolecular disulfide bond, were synthesized using an iodine oxidation strategy (I_2/AcOH) often used for oxidative cyclization. The two homodimeric bactenecins ADB and TDB, which contain an intermolecular disulfide bond, were produced through aqueous oxidative folding (DMSO/AcOH) of reduced linear bactenecin. All of the peptides used in this study are depicted in Table 1 together with their sequences, disulfide bonds, and minimum inhibitory concentration (MIC) values against *S. aureus* and *E. coli*. The monomeric and homodimeric bactenecins tested displayed potent antimicrobial activity with MIC values of 1-8 μM and 2-4 μM, respectively.

Kinetics of the bactericidal activities of bactenecin derivatives and the effect of salt

To discern differences in the mechanisms by which the four bactenecin peptides exert their lethal effects, we initially characterized the kinetics of their bactericidal activities against *S. aureus* and *E. coli*, as representative of Gram-positive and Gram-negative bacteria, respectively. Fig. 1 shows the time-dependent decline in the number of surviving cells (colony forming units (CFU)/mL) with incubation in the presence of each peptide. At a concentration of 8 μM, the homodimeric bactenecins ADB and TDB almost completely killed *S. aureus* within 10 min and *E. coli* within 30 min. Similarly, the monomeric bactenecins MTB and TMB exhibited potent killing kinetics at a concentration of 16 μM, though TMB displayed greater bactericidal activity than MTB against *S. aureus*. This finding is consistent with the earlier finding that insertion of a tryptophan

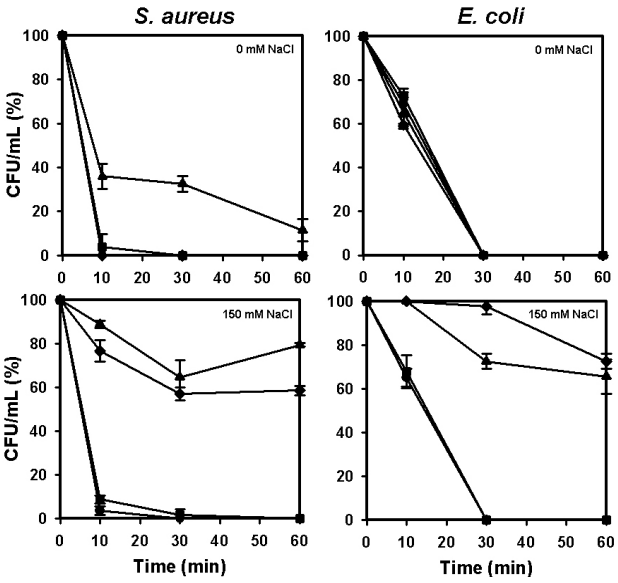

Fig. 1. Bactericidal kinetics of the four bactenecin derivatives against *S. aureus* (left panel) and *E. coli* (right panel). Bacteria treated with the each peptides were diluted at the indicated times and plated on LB agar. The CFUs were counted after 16 h of incubation at 37°C. Values are means ± S.D. of two independent measurements. Symbols: ADB (●, 8 μM); MTB (▲, 16 μM); TDB (■, 8 μM); TMB (◆, 16 μM).

Table 1. The primary structure, disulfide bonding connections and MICs of the peptides used in this study

Peptide	Amino acid sequence	MIC (μM)		Peptide	Amino acid sequence	MIC (μM)	
		S. aureus	*E. coli*			*S. aureus*	*E. coli*
MTB	RLCRIVVIRVCR	4-8	1-2	ADB	NH_2-RLCRIVVIRVCR-CO_2H CO_2H-RCVRIVVIRCLR-NH_2	1-2	1-2
TMB	RLCRIVWIRVCR	2-4	1-2	TDB	NH_2-RLCRIVWIRVCR-CO_2H CO_2H-RCVRIWVIRCLR-NH_2	2-4	2-4

MTB: monomeric turn bactenecin, ADB: antiparallel dimeric bactenecin, TMB: Trp-substituted monomeric bactenecin, TDB: Trp-substituted dimeric bactenecin.

between two valine residues at the center of TMB increased the peptide's potency against Gram-positive bacteria (15).

We next examined the effect on peptide activity of increasing the ionic strength in the environment by adding 150 mM NaCl to the buffer (Fig. 1). We found that the antibacterial activities of the homodimeric bactenecins against both *S. aureus* and *E. coli* were unaffected by the increase in ionic strength, but the activities of the monomeric bactenecins against both bacteria were significantly reduced by >60%. These findings are consistent with those of our earlier study (17) and indicate that dimerization enables the peptides to retain potent bactericidal activity in the presence of physiological levels of salt, and further suggest that the bactericidal mechanisms of tryptophan-containing TDB and TMB are similar to those of ADB and MTB, respectively, which have no intrinsic fluorescence.

Analysis of tryptophan fluorescence and its quenching by acrylamide

Because TDB and TMB display antibiotic profiles similar to ADB and MTB, respectively, we were able to analyze the binding of bactenecins to lipid membranes using these tryptophan-containing derivatives. Measured was tryptophan fluorescence emitted by TDB and TMB in the presence and absence of anionic L-phosphatidylcholine (EYPC)/egg yolk L-phosphatidyl-DL-glycerol (EYPG) (1 : 1) liposomes (Fig. 2). In Tris buffer, the wavelength maxima of TDB and TMB were 347.4 and 349 nm, respectively, which is typical for tryptophan residues in a hydrophilic environment (Table 2). When EYPC/EYPG liposomes were added to TDB- or TMB-containing buffer to the indicated peptide/lipid molar (P/L) ratios, there were significant changes in the tryptophan fluorescence spectra (Fig. 2). Upon addition of the anionic liposomes, both TDB and TMB showed large blue shifts (about 8-12 nm) in their emission maxima, indicating movement of the tryptophan residue from the aqueous buffer into the hydrophobic environment of the liposomes [20]. On the other hand, the two derivatives showed a significant difference in their fluorescence quantum yields. As shown in Fig. 2, increasing the concentration of anionic liposomes in the presence of TMB induced increases in the tryptophan fluorescence intensity, whereas the intensity of the fluorescence from TDB was reduced by 60%. It was previously shown that molecular aggregation of tryptophan-containing peptides can lead to the positioning of tryptophan residues in close proximity to one another, resulting in a reduction in fluorescence intensity due to self-quenching (21-23).

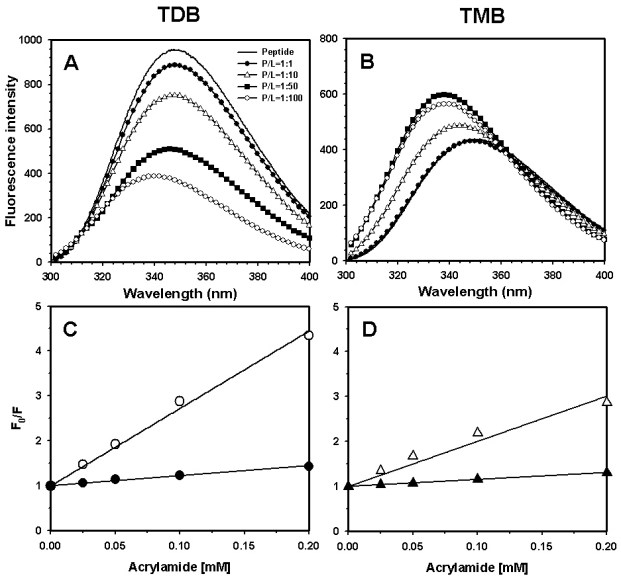

Fig. 2. Trp fluorescence emission spectra and Stern-Volmer plots for the quenching of Trp fluorescence by acrylamide with TDB and TMB. Fluorescence spectra for TDB (A) and TMB (B) were recorded at increasing concentrations of EYPC/EYPG (1 : 1) liposomes in Tris buffer (pH 7.4) at 25°C. Quenching assays for TDB (C, ● and ○) and TMB (D, ▲ and △) were carried out in buffer (empty symbols) and at a molar peptide/lipid ratio of 1 : 100 [EYPC/EYPG (1 : 1), filled symbols].

In an earlier study, we also found that homodimeric bactenecin undergoes oligomerization on tricine-acrylamide gel (17). This prompted us to further investigate the membrane-integrated state of TDB and TMB by carrying out a fluorescence quenching experiment using the neutral quencher acrylamide. From the Stern-Vlomer plots characterizing the quenching of tryptophan fluorescence (Fig. 2), we derived the apparent Stern-Volmer quenching constants (K_{sv}), which are presented in Table 2. In aqueous buffer, the fluorescent emission from TDB and TMB was proportionally quenched with increases in the acrylamide concentration, which means the tryptophan residue was fully exposed with no intermolecular aggregation. As shown in Fig. 2, however, in the presence of the liposomes at a P/L ratio of 1 : 100, the fluorescence intensity of both TDB and TMB was less sensitive to increases in the acrylamide concentration. Moreover, the estimated K_{sv} values for TDB and TMB in aqueous buffer were about 10-fold larger than in the presence of the liposomes (Table 2). It thus appears that in the presence of liposomes, the tryptophan residues in both homodimeric and monomeric bactenecins are buried fairly deeply in the lipid bilayer, making them less accessible to acrylamide.

Release of dye leakage from liposomes

To gain a better understanding of their mechanisms of action,

Table 2. λ_{max} (nm) of tryptophan fluorescence emission and the Stern-Volmer quenching constants (K_{sv}) in the presence of liposomes

Peptide	λ_{max} (nm)		K_{sv}	
	Tris buffer	PC/PG (1/1)	Tris buffer	PC/PG (1/1)
TDB	347.4	339.2 (8.2)*	17.23	2.24
TMB	349	336.8 (12.2)	10.06	1.55

*Blue shift of emission maxima, as compared to Tris buffer.

we next tested whether MTB or ADB form a pore in the bacterial membrane, or whether either acts as a detergent. This entailed measuring the peptide-induced release of calcein (623 Da) or fluorescently labeled dextran dyes [FD-4 (3.9 kDa, 1.4 nm), FD-40 (40.5 kDa, 4.45 nm) and FD-500 (530 kDa, 14.7 nm)] from EYPC/EYPG (1 : 1) liposomes, after which the relative lytic efficiency of the peptides was determined by comparison with the release induced by Triton X-100, which completely disrupted the vesicles (Fig. 3). In the calcein release assay, MTB (10 μM) induced relatively little release from liposomes (~20%), whereas ADB (5 μM) displayed somewhat greater membrane-lytic activity (~60%), suggesting membrane disruption is an important lethal effect of ADB. In the dextran release assays, MTB (10 μM) induced little or no release of any of the three dextran dyes from liposomes. By contrast, ADB (5 μM) again displayed substantial membrane-lytic activity, inducing about 40-50% release of FD-4 and FD-40 from liposomes and less than 20% release of FD-500. It is noteworthy that ADB's ability to induce leakage through model membranes was dependent on dye size, and gradually declined as the size of the dye molecule increased. Considering the size of the dyes used, it seems likely that ADB forms pores, ranging from 1.4 nm to 14.7 nm in diameter, at a P/L ratio of 1/20. On the basis of these results, we suggest that ADB rapidly exerts a potent antibacterial effect by forming pores through oligomerization on the lipid membrane and that MTB exerts its antibacterial effect in some other way.

Cytoplasmic membrane depolarization

To investigate whether the ability of antibacterial peptides to induce leakage through model membranes correlates with their antibacterial activity, we evaluated the effects of bactenecin peptides on *S. aureus* cytoplasmic membranes using the membrane potential-sensitive fluorescent dye $diSC_3(5)$ (Fig. 4).

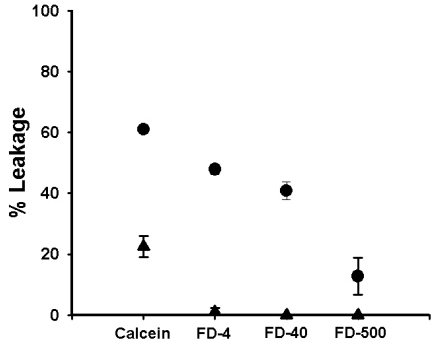

Fig. 3. Peptide-induced release of calcein and FITC-dextrans (FD) of various size from EYPC/EYPG (1 : 1) liposomes. Liposomes (100 μM) containing calcein, FD4, FD40 or FD-500 were incubated in the presence of ADB (5 μM, ●) or MTB (10 μM, ▲) for 5 min at room temperature. Fluorescence from liposomes lysed with Triton X-100 served as an indicator of 100% release. Values are the means ± S.D. of two independent measurements.

This dye is distributed between the cells and the medium in a manner that is dependent on the cytoplasmic membrane potential. When potential is high, the dye is concentrated inside bacterial cells, and self-quenching diminishes the dye's fluorescence. Upon membrane depolarization, however, the dye is released into the medium, causing a measurable increase in fluorescence. As shown in Fig. 4A, addition of ADB resulted in an increase in $diSC_3(5)$ fluorescence reflecting membrane depolarization, after which addition of gramicidin D fully collapsed the membrane potential. Interestingly, ADB and MTB showed considerable differences in their ability to depolarize the membrane. ADB rapidly and dose-dependently depolarized the *S. aureus* cytoplasmic membrane, and caused complete depolarization at a concentration one-fourth that of its MIC value (0.5 μM) (Fig. 4B). By contrast, MTB had no detectable ability to depolarize the *S. aureus* membrane, even at a concentration of 32 μM. Likewise, MTB also reportedly has a negligible effect on membrane potential in *E. coli* DC cells

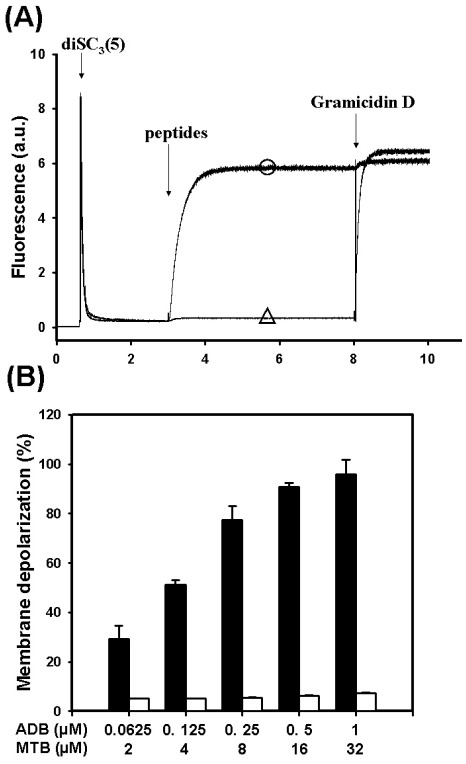

Fig. 4. Effect of ADB and MTB on the cytoplasmic membrane potential in intact *S. aureus* cells. Once the fluorescence had stabilized after addition of the membrane potential-sensitive dye $diSC_3(5)$ (20 nM) to a suspension of *S. aureus* cells (OD_{600} = 0.05), the peptide of interest was added. Gramicidin D (0.22 nM) was used to fully collapse the membrane potential. (A) Time-dependent effects of ADB (○, 0.5 μM) and MTB (△, 32 μM). (B) Concentration-dependent effect of ADB (0.0625-1 μM, filled bars) and MTB (2-32 μM, empty bars). Values are normalized to the effect of Gramicidin D, which was assigned a value of 100%.

(18). Taken together, these results suggest that whereas ADB likely acts by forming a pore in the bacterial membrane, MTB likely acts by penetrating through the membrane to target intracellular molecules or organelles.

It was recently reported that dimerization of the cell-penetrating peptides Tat and penetration induces a significant change in the mode of their action: the monomeric forms target intracellular molecules/organelles, while the dimeric forms target the cell membrane (24, 25). This functional switch from intracellular to membrane targeting is quite similar to what we observed with monomeric and homodimeric bactenecin in the present study. With respect to the secondary structure, however, both the monomeric and dimeric forms of penetration assume an α-helical structure in a membrane-mimicking environment. By contrast, the monomeric and dimeric forms of bactenecin assume β-hairpin and β-sheet-like structures, respectively.

In sum, our results suggest that dimerization of peptides rich in basic amino acids could represents a powerful means of inducing strong interaction with the cellular membrane compartment, irrespective of the secondary structure. Moreover, they may serve as a template for the design of therapeutic agents able to tolerate physiological salt concentrations.

MATERIALS AND METHODS

Materials

Fluoren-9-yl-methoxycarbonyl (Fmoc)-amino acids and other reagents used for peptide synthesis were purchased from Calbiochem-Novabiochem (La Jolla, CA). Egg yolk L-phosphatidylcholine (EYPC), egg yolk L-phosphatidyl-DL-glycerol (EYPG), calcein, fluorescein isothiocyanate (FITC)-labeled dextrans (FD-4, FD-40 and FD-500) and gramicidin D were supplied by Sigma Chemical Co. (St. Louis, MO). 3,3'-Dipropylthiadicarbocyanine iodide (diSC_3(5)) was from Molecular Probes (Eugene, OR). All other reagents were of analytical grade. The buffers were prepared in double glass-distilled water.

Peptide design, synthesis and characterization

All peptides were synthesized using the solid-phase peptide synthesis method performed manually with Fmoc chemistry. The peptides were cleaved from the resin using trifluoroacetic acid containing various scavengers and purified by preparative RP-HPLC (Shimadzu, Tokyo, Japan). As previously reported (17), oxidation of 1 mM reduced linear bactenecin or its Trp-substituted linear analog in buffer solution containing 2 M acetic acid (AcOH)/H_2O/dimethylsulfoxide (DMSO) (1 : 2 : 1, v/v) for 24 h at room temperature with gentle stirring yielded ADB or TDB, respectively. MTB and TMB exhibiting a β-hairpin conformation were oxidized in AcOH/H_2O (4 : 1, v/v), which was followed by addition of iodine (10 equivalents to the number of disulfide bonds). The correctness of the masses of the synthetic peptides was confirmed by MALDI-TOF MS (Shimadzu, Tokyo, Japan). In addition, trypsin digestion of TDB confirmed that, like ADB, TDB is antiparallel (data not shown).

Antimicrobial activity and kinetics

The antimicrobial activity of the peptides was examined in sterile 96-well plates (Falcon) in a final volume of 100 μL. Aliquots (50 μL) of a bacterial suspension at 2×10^5 CFU/mL in culture medium (1% peptone) were added to 50 μL of aqueous peptide solution (serial 2-fold dilutions in 1% peptone). After incubation for 18-20 h at 37°C, the inhibition of bacterial growth was assessed by measuring the absorbance at 620 nm using a Microplate Autoreader EL 800 (Bio-tek Instruments). The MIC was defined as the lowest concentration of peptide that inhibited growth.

To evaluate the kinetics of the antimicrobial activity of the peptides, Gram-positive *S. aureus* (KCTC 1621) and Gram-negative *E. coli* (KCTC 1682) were grown to mid-log phase at 37°C in Luria Bertani medium. The cells were then diluted to give approximately 2×10^6 CFU/mL, after which they were treated with 8 μM ADB or TDB or with 16 μM MTB or TMB. After 0, 10, 30 or 60 min of exposure to the peptides at 37°C, 50 μL aliquots of serial 10-fold dilutions (up to 10^{-3}) of the cultures were plated onto LB agar plates to assess their viability. Colonies were counted after incubation for 16 h at 37°C. The results of two independent experiments were averaged.

Preparation of large and small unilamellar vesicles

For calcein release experiments, large unilamellar vesicles (average diameter, 100 nm) containing the fluorescent probe calcein were prepared by extrusion. Phospholipids composed of EYPC/EYPG (1 : 1, w/w) were dissolved in chloroform and then dried using a rotary evaporator to form a thin lipid film. The lipid film was then further dried overnight under vacuum before being hydrated with Tris/HCl buffer (10 mM Tris, 150 mM NaCl, 1 mM EDTA, pH 7.4) or 70 mM calcein solution and vortex mixed. The resultant suspensions were subjected to five freeze-thaw cycles and then pressure-extruded through polycarbonate filters (LiposoFast, 0.1 μm pore size, 20 times). Vesicles containing entrapped calcein were separated from free calcein by gel filtration on Sephadex G-50 columns (Pharmacia, Uppsala, Sweden) equilibrated with Tris/HCl buffer.

Small unilamellar vesicles used for Trp fluorescence and quenching experiments were prepared by sonication. The dried lipid film was hydrated with 10 mM Tris buffer (pH 7.4) by vortex mixing. Using a titanium-tipped sonicator, the resultant suspension was then sonicated in an ice bath for about 20 min, until it was clear. Thereafter, dynamic light-scattering experiments confirmed the presence of a main population of vesicles (>96% mass content) with a mean diameter of 42 nm.

Trp fluorescence and quenching by acrylamide

Measurements of tryptophan fluorescence were made using a Shimadzu RF-5301 spectrofluorometer. EYPC/EYPG (1 : 1, w/w) liposomes were added to a fixed concentration of TDB (1 μM) or TMB (3 μM) dissolved in 3 mL of Tris buffer until the desired P/L ratio was reached, after which the tryptophan residue

in the peptide was excited at 280 nm (band width, 5 nm), and the emission spectrum was recorded from 300 to 400 nm (band width, 3 nm). Acrylamide quenching experiments were carried out using an excitation wavelength of 295 nm instead of 280 nm to reduce absorbance by acrylamide. Trp fluorescence was quenched by titration with acrylamide from a 4 M stock solution to a final concentration of 0.2 M in the presence of liposomes at a P/L ratio of 1 : 100. The quenching data were plotted according to the Stern-Volmer equation $F_0 / F = 1 + K_{sv}[Q]$, where F_0 is the fluorescence of the peptide in the absence of acrylamide, F is the fluorescence of the peptide in the presence of acrylamide, K_{sv} is the Stern-Volmer quenching constant and [Q] is the concentration of acrylamide.

Calcein release assays

The fluorescence of calcein released from liposomes was monitored at 520 nm (excited at 490 nm) on a Shimadzu RF-5301 spectrofluorometer. To induce 100% leakage, 10% w/v Triton X-100 (20 μL) was added, which destroyed the vesicles. The percentage of the dye caused to leak from the liposomes by the peptides was calculated using the equation% leakage = $100 \times (F / F_0) / (F_t / F_0)$, where F_0 and F_t are the initial fluorescence intensities observed without the peptides and after Triton X-100 treatment, respectively, and F is the fluorescence intensity achieved with the peptides.

Preparation of dextran-loaded liposomes and leakage assay

FITC-labeled dextrans with the indicated molecular weights (FD-4, FD-40, and FD-500) were utilized as model cytoplasmic components. Dextran-loaded PG/PC (1 : 1) liposomes containing FITC were prepared using the reverse-phase evaporation method (26). A buffer solution (PBS buffer) containing 2 mg/mL FITC-labeled dextran was sonicated for 15 min with a lipid solution in chloroform (20 mg/mL) at 0-5°C, at which time the mixture had become an homogeneous opalescent dispersion. The mixture was then placed on a rotary evaporator, and the chloroform was removed by rotation at approximately 200 rpm at 20°C. As it became an aqueous suspension with the removal of the chloroform, buffer (2 mL) was added, and the suspension was evaporated for an additional 15 min at 20°C to further remove the traces of organic solvent. The preparation was then centrifuged for 30 min at 22,000 × g and washed several times to remove unencapsulated material and any residual organic solvent. Aliquots of the resultant peptide solutions at appropriate concentrations were then incubated with a suspension of FD-loaded liposomes (100 μM) for 10 min at 25°C, after which they were centrifuged for 30 min at 22,000 × g, the supernatants were recovered, and leakage was recorded by monitoring the FITC fluorescence intensity (excitation wavelength: 490 nm, emission wavelength: 520 nm). One hundred percent leakage was achieved by addition of 20 μL of 10% Triton X-100. The percent leakage values were then plotted.

Membrane depolarization assay

Measurements of cytoplasmic membrane depolarization were made using a membrane potential-sensitive probe, 3,3′-dipropylthiacarbocyanine [diSC$_3$(5)] as previously described (10). *Staphylococcus aureus* (KCTC 1621) was grown at 37°C to mid-log phase, centrifuged (3,000 rpm, 3 min) and washed three times with 5 mM HEPES buffer (pH 7.2) containing 20 mM glucose and resuspended in buffer (5 mM HEPES, 20 mM glucose, 100 mM KCl, pH 7.2) to an OD_{600} of 0.05. Changes in fluorescence due to the collapse of the cytoplasmic membrane potential were continuously monitored at 25°C using a RF-5301 spectrofluorometer (Shimadzu, Tokyo, Japan) at an excitation wavelength of 622 nm and an emission wavelength of 670 nm. Peptides were added to the cells when the dye uptake was maximal, which was indicated by a stable reduction in fluorescence due to quenching of the accumulated dye in the membrane interior. Complete dissipation of the *S. aureus* cell membrane potential was accomplished using gramicidin D (0.22 nM), which forms ion channels in the cytoplasmic membrane of the bacteria. Measurements were repeated twice under each condition to ensure reproducibility.

REFERENCES

1. Zasloff, M. (2002) Antimicrobial peptides of multicellular organisms. *Nature* **415**, 389-395.
2. Andreu, D. and Rivas, L. (1998) Animal antimicrobial peptides: an overview. *Biopolymers* **47**, 415-433.
3. Koczulla, A. R. and Bals, R. (2003) Antimicrobial peptides: current status and therapeutic potential. *Drugs* **63**, 389-406.
4. Matsuzaki, K. (2008) Control of cell selectivity of antimicrobial peptides. *Biochim. Biophys. Acta* (in press).
5. Brogden, K. A. (2005) Antimicrobial peptides: pore formers or metabolic inhibitors in bacteria? *Nat. Rev. Microbiol.* **3**, 238-250.
6. Yeaman, M. R. and Yount, N. Y. (2003) Mechanisms of antimicrobial peptide action and resistance. *Pharmacol. Rev.* **55**, 27-55.
7. Papo, N. and Shai, Y. (2003) Can we predict biological activity of antimicrobial peptides from their interactions with model phospholipid membranes? *Peptides* **24**, 1693-1703.
8. Shai, Y. (2002) Mode of action of membrane active antimicrobial peptides. *Biopolymers* **66**, 236-248.
9. Cudic, M. and Otvos, L. Jr. (2002) Intracellular targets of antibacterial peptides. *Curr. Drug Targets* **3**, 101-106.
10. Yang, S. T., Shin, S. Y., Hahm, K. S. and Kim, J. I. (2006) Different modes in antibiotic action of tritrpticin analogs, cathelicidin-derived Trp-rich and Pro/Arg-rich peptides. *Biochim. Biophys. Acta* **1758**, 1580-1586.
11. Podda, E., Benincasa, M., Pacor, S., Micali, F., Mattiuzzo, M., Gennaro, R. and Scocchi, M. (2006) Dual mode of action of Bac7, a proline-rich antibacterial peptide. *Biochim. Biophys. Acta* **1760**, 1732-1740.
12. Romeo, D., Skerlavaj, B., Bolognesi, M. and Gennaro, R. (1988) Structure and bactericidal activity of an antibiotic

dodecapeptide purified from bovine neutrophils. *J .Biol. Chem.* **263**, 9573-9575.
13. Wu, M. and Hancock, R. E. W. (1999) Interaction of the cyclic antimicrobial cationic peptide bactenecin with the outer and cytoplasmic membrane. *J. Biol. Chem.* **274**, 29-35.
14. Gennaro, R., Skerlavaj, B. and Romeo, D. (1989) Purification, composition, and activity of two bactenecins, antibacterial peptides of bovine neutrophils. *Infect. Immun.* **57**, 3142-3146.
15. Wu, M. and Hancock, R. E. W. (1999) Improved derivatives of bactenecin, a cyclic dodecameric antimicrobial cationic peptide. *Antimicrob. Agents Chemother.* **43**, 1274-1276.
16. Storici, P., Tossi, A., Lenarcic, B. and Romeo, D. (1996) Purification and structural characterization of bovine cathelicidins, precursors of antimicrobial peptides. *Eur. J. Biochem.* **238**, 769-776.
17. Lee, J. Y., Yang, S. T., Lee, S. K., Jung, H. H., Shin, S. Y., Hahm, K. S. and Kim, J. I. (2008) Salt-resistant homodimeric bactenecin, a cathelicidin-derived antimicrobial peptide. *FEBS J.* **275**, 3911-3920.
18. Wu, M., Maier, E., Benz, R. and Hancock, R. E. W. (1999) Mechanism of interaction of different classes of cationic antimicrobial peptides with planar bilayers and with the cytoplasmic membrane of Escherichia coli. *Biochemistry* **38**, 7235-7242.
19. Lakoxicz, J. R. (1999) Principles of Fluorescence Spectroscopy, 2nd ed., Kluwer Academic/Plenum, New York, USA.
20. Zelezetsky, I., Pontillo, A., Puzzi, L., Antcheva, N., Segat, L., Pacor, S., Crovella, S. and Tossi, A. (2006) Evolution of the primate cathelicidin. Correlation between structural variations and antimicrobial activity. *J. Biol. Chem.* **281**, 19861-19871.
21. Breukink, E., van Kraaij, C., van Dalen, A., Demel, R. A., Siezen, R. J., de Kruijff, B. and Kuipers, O. P. (1998) The orientation of nisin in membranes. *Biochemistry* **37**, 8153-8162.
22. Zhao, H. and Kinnunen, P. K. (2002) Binding of the antimicrobial peptide temporin L to liposomes assessed by Trp fluorescence. *J. Biol. Chem.* **277**, 25170-25177.
23. Christiaens, B., Symoens, S., Verheyden, S., Engelborghs, Y., Joliot, A., Prochiantz, A., Vandekerckhove, J., Rosseneu, M. and Vanloo, B. (2002) Tryptophan fluorescence study of the interaction of penetratin peptides with model membranes. *Eur. J. Biochem.* **269**, 2918-2926.
24. Zhu, W. L. and Shin, S. Y. (2009) Effects of dimerization of the cell-penetrating peptide Tat analog on antimicrobial activity and mechanism of bactericidal action. *J. Pept. Sci.* **15,** 345-352.
25. Zhu, W. L. and Shin, S. Y. (2009) Antimicrobial and cytolytic activities and plausible mode of bactericidal action of the cell penetrating peptide penetratin and its lys-linked two-stranded peptide. *Chem. Biol. Drug Des.* **73**, 209-215.
26. Szoka, F. Jr. and Papahadjopoulos, D. (1978) Procedure for preparation of liposomes with large internal aqueous space and high capture by reverse-phase evaporation. *Proc. Natl. Acad. Sci. U.S.A.* **75**, 4194-4198.